Supporting Information

Stabilizing $Li_{1.3}Al_{0.3}Ti_{1.7}(PO_4)_3$/Li metal anode interface in solid-state batteries by LiF/Cu-rich multifunctional interlayer

1. Experimental Section

1.1 Preparation of LATP

$Li_{1.3}Al_{0.3}Ti_{1.7}(PO_4)_3$ (LATP) solid electrolyte was prepared by a traditional solid-state sintering method through weighing of Li_2CO_3 (99%, Aladdin), Al_2O_3 (99.99%, Aladdin), TiO_2 (99.8%, Aladdin) and $NH_4H_2PO_4$ (99%, Merck) according to stoichiometric ratio. An excess of 10 wt% Li_2CO_3 was added to compensate for the loss of lithium during the sintering process. After grinding at 400 rpm for 9 h, the mixture was calcined at 900 °C in air for 2 h to obtain the LATP powder. In order to reduce the particle size, the LATP powder was ball milled at 400 rpm for 9 h. The LATP powder after ball milling was pressed at 8 MPa for 10 min. The pressed ceramic sheets were covered with LATP powders and sintered in 850 °C air at 2 °C/min for 4 h to obtain the dense LATP pellets.

1.2 Preparation of CuF_2 composite layer

0.125 g polyvinylidene fluoride (PVDF, Aladdin) and 0.05 g LiTFSI ($LiC_2F_6NO_4S_2$, 99.9%, Aladdin) were dissolved in 4 mL 1, 2-Dimethoxyethane (DME). CuF_2 powder (99.5%, Aladdin) (0.011 g, 0.025 g and 0.048 g, corresponding to 5 wt%, 10 wt% and 15 wt% CuF_2) and $LiNO_3$ (99.9%, Aladdin) (0.022 g, 0.050 g and 0.096 g) with a weight ratio of 1: 2 were added into the above solution and then magnetically stirred for 12 h to obtain a mixed solution. LiTFSI is used to form a polymer-salt mixture with PVDF, and also can increase ionic conductivity of the interlayer. $LiNO_3$ was employed to

increase the solubility of CuF_2 in DME solvent. A drop of ~20 μL mixed solution was coated on the surface of LATP pellets and then dried naturally for 2 h. The other side was applied in the same way to obtain CuF_2@LATP. All of the above processes were performed in the glove box. In order to investigate the effect of CuF_2 layer with different thicknesses on the electrochemical performance, the CuF_2 layer with different thicknesses were prepared by varying the amount of 10 wt% CuF_2 solution (10 μL, 20 μL and 30 μL).

1.3 Characterizations

The prepared LATP pellets were characterized by X-ray diffractometer (XRD, Ultima IV, Rigaku) under 40 kV and 40 mA Cu-kα radiation (10°~80°). Scanning electron microscopy (SEM, JSM-7500F JEOL) and energy dispersive spectrometer (EDS) were used to study the surface, cross-section morphology and element distribution of LATP pellets and lithium metal anodes. The composition and valence states have been analyzed by X-ray photoelectron spectroscopy (XPS) measurements made by PHI Quantera II, Japan.

1.4 Electrochemical Tests

To assemble lithium symmetric batteries, lithium foil is used as electrode, CuF_2@LATP or LATP are employed as electrolyte. To assemble the full battery, cathode material ($LiFePO_4$ or $LiNi_{0.8}Co_{0.1}Mn_{0.1}O_2$) (LFP or NCM), conductive additive (Super P), and binder (PVDF) with weight ratio of 8:1:1 were dispersed in N-methyl pyrrolidone (NMP). The obtained slurry was coated on aluminum foil, and the active material loading was 1.2-1.5 mg cm^{-2}. It was placed into a 110 ^oC vacuum oven for 12 h. The dried coated aluminum foil was punched into small circles. LFP or NCM and Li foil were used as cathode and anode, respectively, and CuF_2@LATP or LATP was used as

solid electrolyte. To ensure good transport of Li^+ across the LFP/LATP or NCM/LATP interfaces, 4 μL of electrolyte (1 M $LiPF_6$ in EC: DMC = 1:1) was added to the cathode side. Finally, the battery was assembled in the Ar filled glove box (MIKROUNA, Super 1220/750, $H_2O \leq 1$ ppm, $O_2 \leq 1$ ppm) using CR2025 configuration.

The ionic conductivity of LATP pellet, the interfacial impedance of symmetric and full batteries were measured via the AC impedance technique (CHI614C electrochemical workstation) in a frequency range from 1 M Hz to 1 Hz with an amplitude of 0.01 V. As for electronic conductivity via the chronoamperometry technique, the constant voltages of 1 V, 2 V, 3 V were applied and the response currents were detected. A silver paste was applied on the surface of LATP pellet as a blocking electrode. The Neware battery test system (CT-4008 T, 5 V/10 mA) was used to perform constant current cycling of symmetric and full batteries at different current densities. Galvanostatic charge-discharge tests for the symmetric batteries were carried out at 0.1, 0.2, and 0.3 mA cm^{-2}, and each cycle was lasted for 2 h. The critical current density (CCD) of the symmetric battery was measured under Time-constant mode, under a fixed cycling period, the areal capacity of Li plating or striping gradually increases (1 h per half-cycle). In the potential range of 2.4 - 4.2 V (LFP, 1 C = 170 mAh g^{-1}) and 2.8 - 4.3 V (NCM, 1 C = 180 mAh g^{-1}), the full batteries were charged and discharged at different current rates (0.1, 0.2, 0.5 and 1.0 C). All electrochemical measurements were performed at 25 ^oC.

2. Supplementary Figures

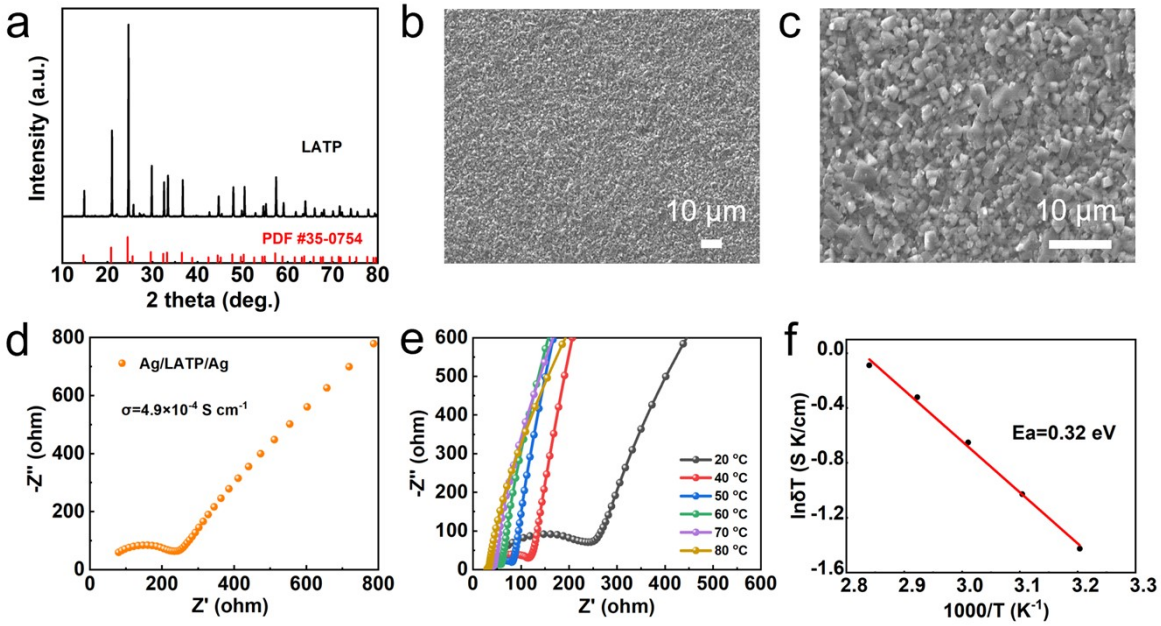

Figure S1. (a) XRD pattern, (b) surface and (c) cross-section SEM images of LATP pellet; (d) EIS curve of the Ag/LATP/Ag electrode; the ionic conductivity of the LATP pellet is 4.9×10^{-4} S cm^{-1}; (e) EIS curves of the Ag/LATP/Ag electrode at different temperatures; (f) Arrhenius plots and the calculated active energy for LATP electrolyte.

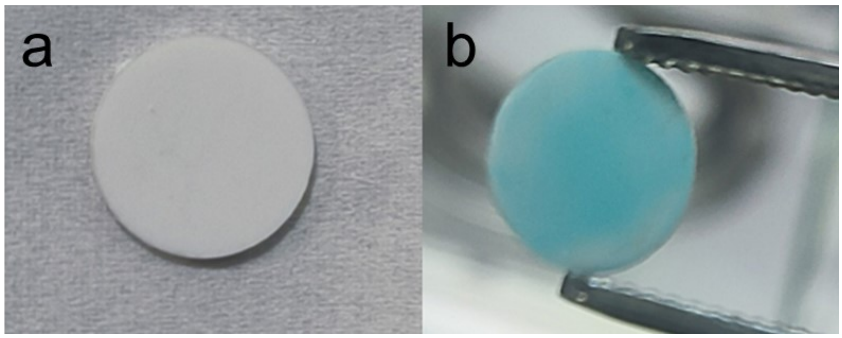

Figure S2. Digital photos of the (a) original LATP and (b) CuF_2@LATP.

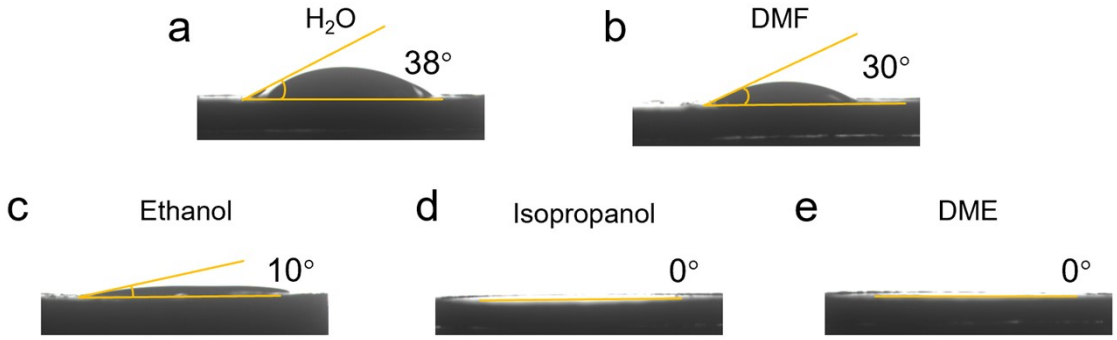

Figure S3. Contact angle measurements of various solution on LATP pellets. (a) H_2O, (b) N, N-Dimethylformamide, (c) Ethanol, (d) Isopropanol and (e) 1, 2-Dimethoxyethane.

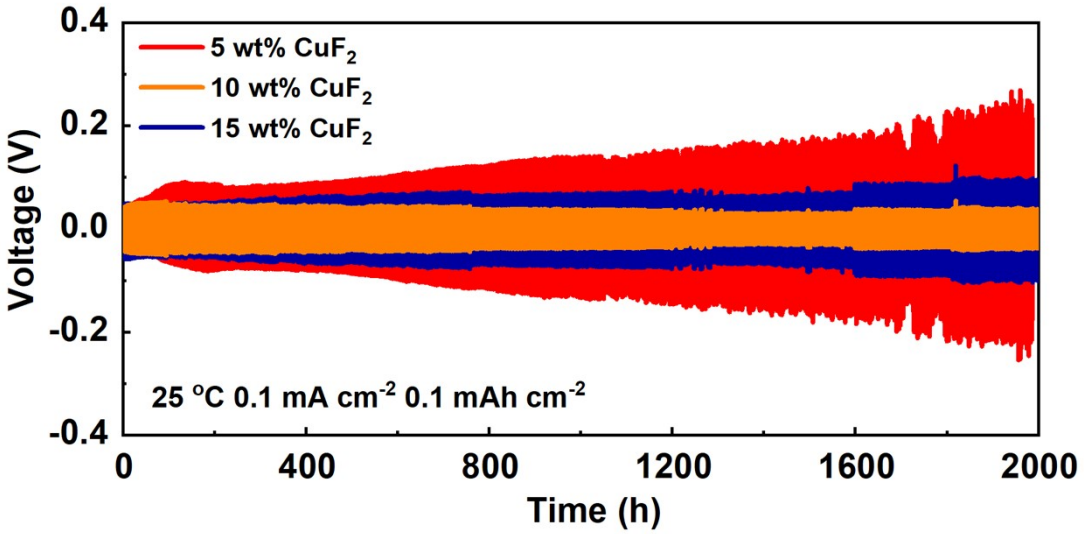

Figure S4. Voltage-time curves of LATP symmetric batteries assembled with different mass ratios of CuF_2 at 0.1 mA cm^{-2}/0.1 mAh cm^{-2}.

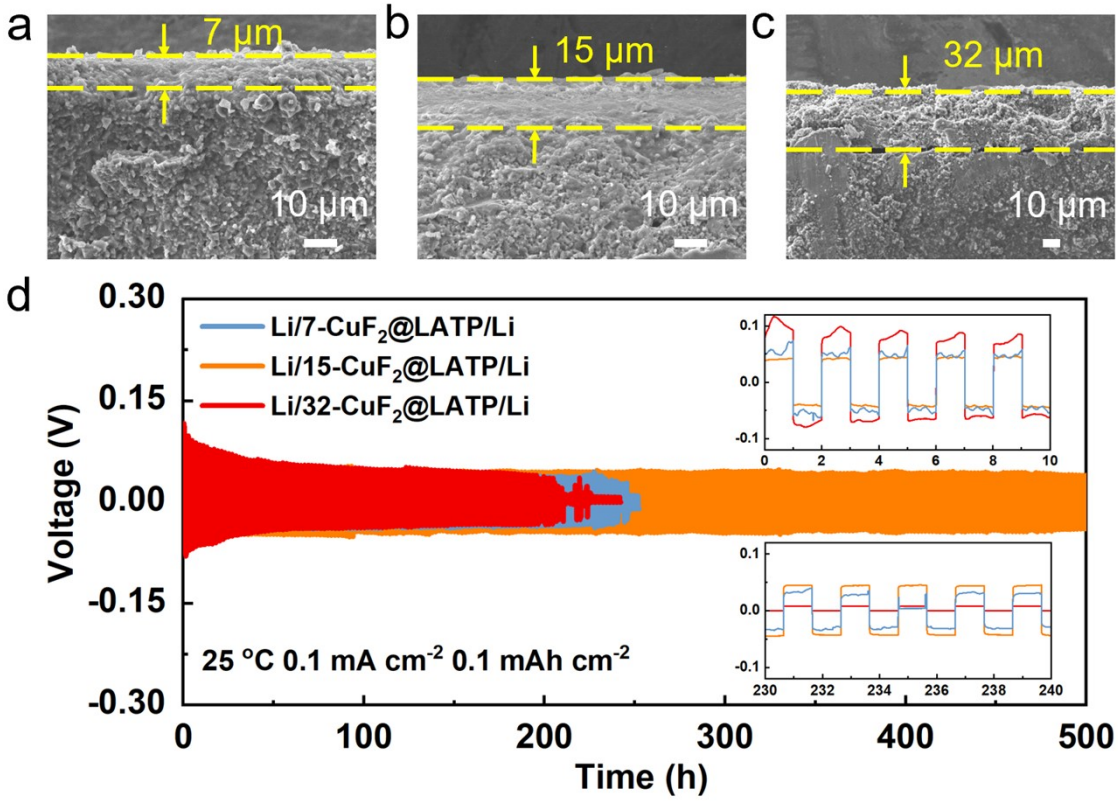

Figure S5. The cross-section SEM images of LATP with CuF_2 composite layer with different thicknesses of (a) 7 μm, (b) 15 μm and (c) 32 μm. (d) Voltage-time curves of LATP symmetric batteries assembled with different thicknesses of CuF_2 composite layer at 0.1 mA cm^{-2}/0.1 mAh cm^{-2}.

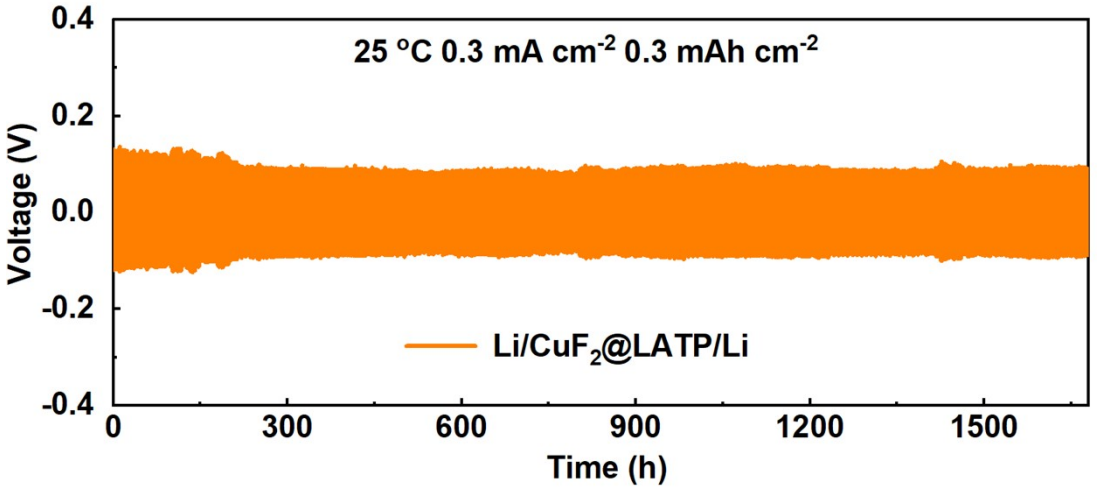

Figure S6. Voltage-time curve of Li/CuF_2@LATP/Li symmetric battery at 0.3 mA cm^{-2}/0.3 mAh cm^{-2}.

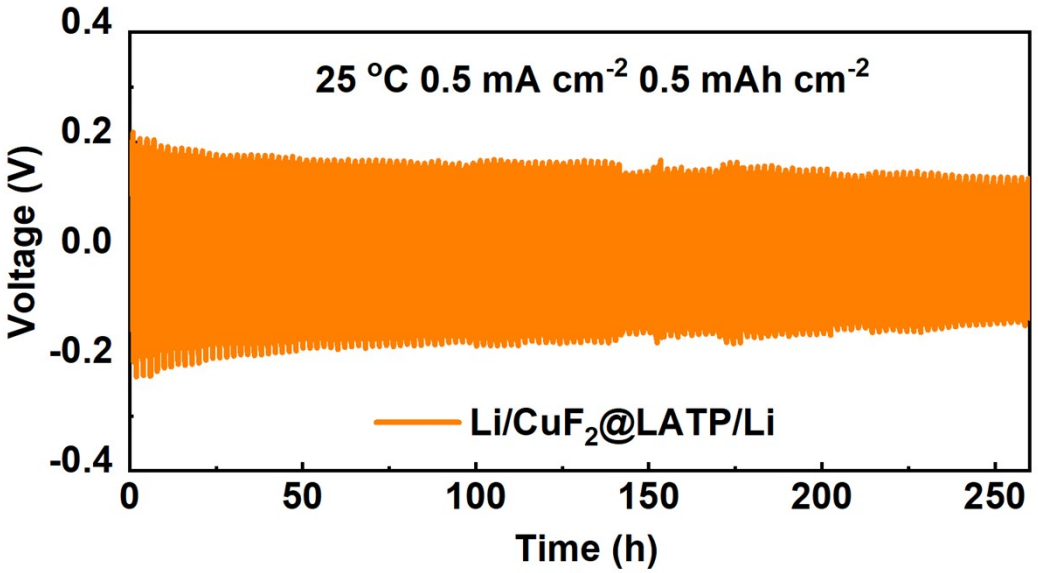

Figure S7. Voltage-time curve of Li/CuF_2@LATP/Li symmetric battery at 0.5 mA cm^{-2}/0.5 mAh cm^{-2}.

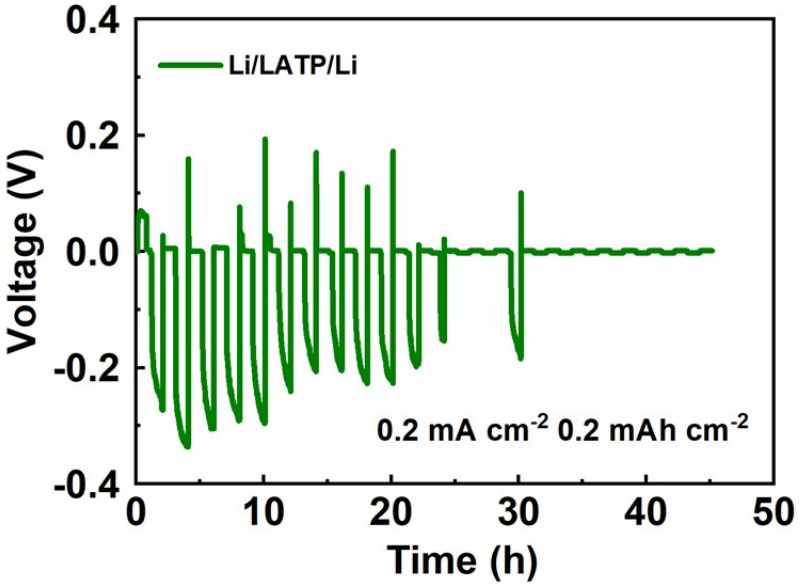

Figure S8. Voltage-time curve of Li/LATP/Li symmetric battery at 0.2 mA cm^{-2}/0.2 mAh cm^{-2}.

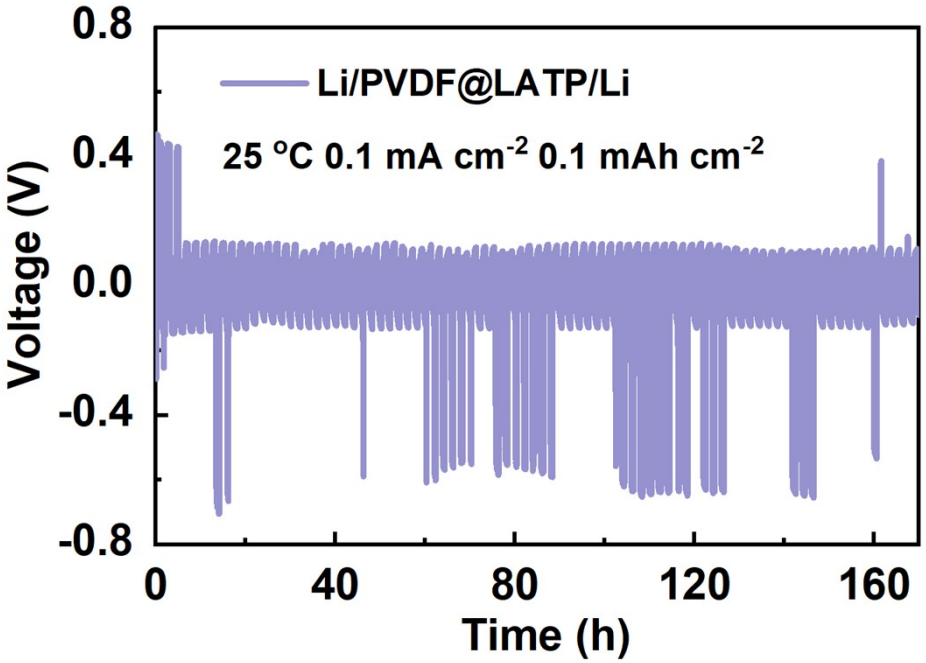

Figure S9. Voltage-time curve of Li/PVDF@LATP/Li symmetric battery at 0.1 mA cm^{-2}/0.1 mAh cm^{-2}.

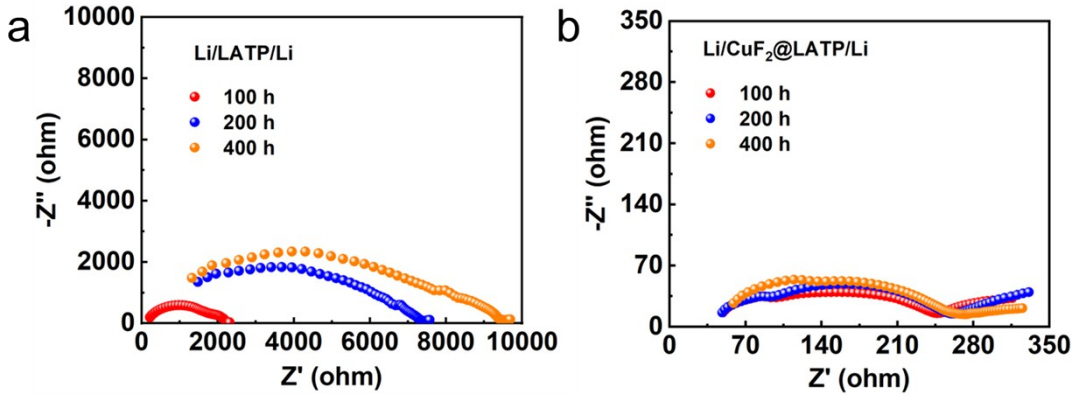

Figure S10. EIS curves of (a) Li/LATP/Li and (b) Li/CuF_2@LATP/Li symmetrical batteries after different cycling time at 0.1 mA cm^{-2}/0.1 mAh cm^{-2}.

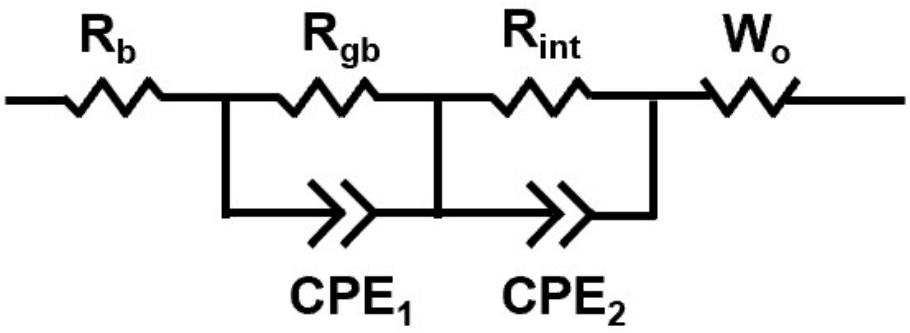

Figure S11. The equivalent circuit of symmetric batteries.

The equivalent circuit of a symmetrical battery, where R_b represents the total resistance of elements such as LATP, interlayer, electrode, and packaging material. R_{gb}, R_{int}, and W_o represent the grain boundary resistance of the LATP, the interfacial resistance between Li and LATP, and the Warburg resistance, respectively.

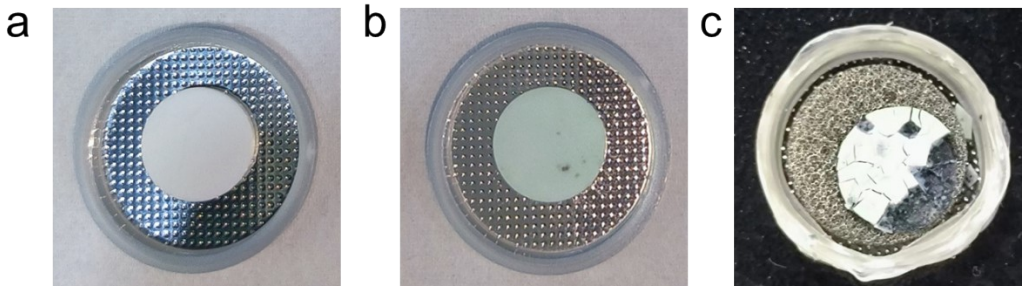

Figure S12. Digital photos of the (a) original LATP pellet, (b) CuF_2@LATP after 100 cycles and (c) LATP after 100 cycles.

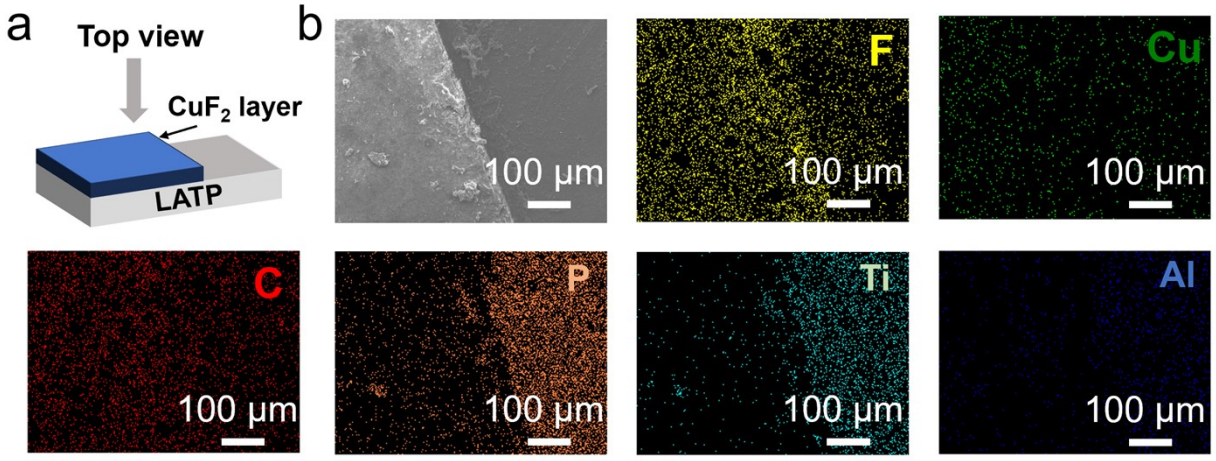

Figure S13. (a) Schematic illustration of CuF_2@LATP. (b) Surface SEM and corresponding EDS mapping images of CuF_2@LATP after 100 cycles.

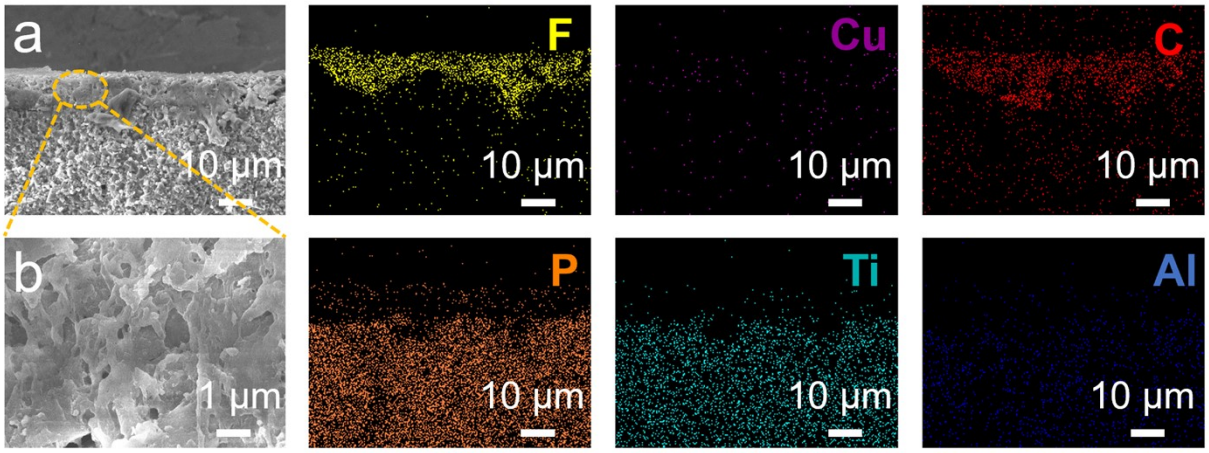

Figure S14. (a) Cross-sectional SEM and corresponding EDS mapping images of CuF_2@LATP after 100 cycles. (b) Magnifying cross-sectional SEM image.

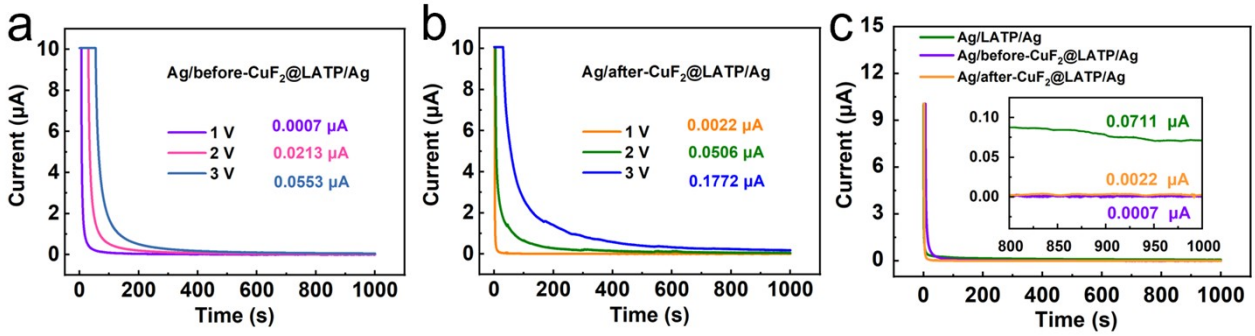

Figure S15. Chronoamperometry curves of (a) Ag/before-CuF_2@LATP/Ag and (b) Ag/after-CuF_2@LATP/Ag electrodes with instant applied external voltages of 1 V, 2 V, 3 V; Chronoamperometry curves of (c) Ag/LATP/Ag, Ag/before-CuF_2@LATP/Ag and Ag/after-CuF_2@LATP/Ag electrodes with an instant applied external voltage of 1 V.

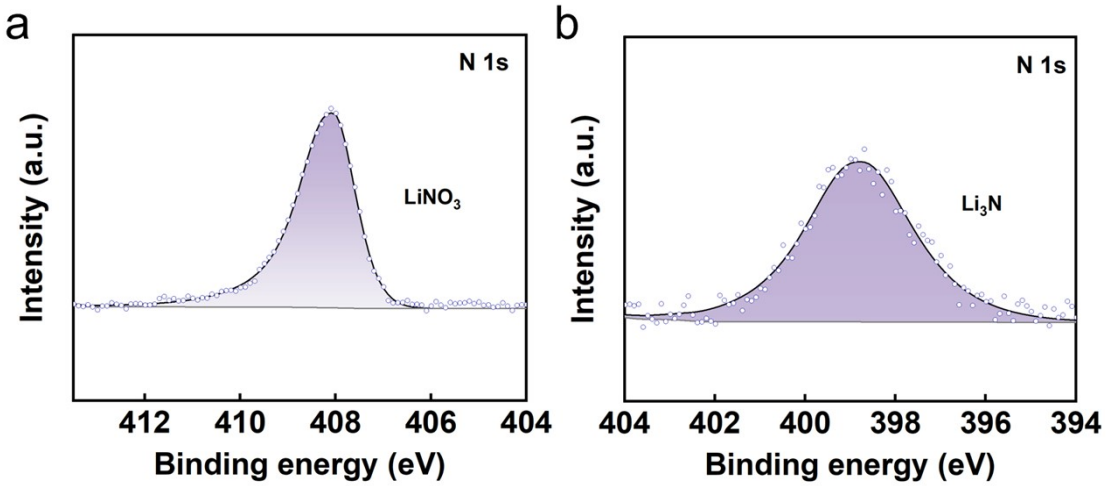

Figure S16. N 1s XPS spectra of CuF_2@LATP surface (a) before cycling and (b) after 100 cycles.

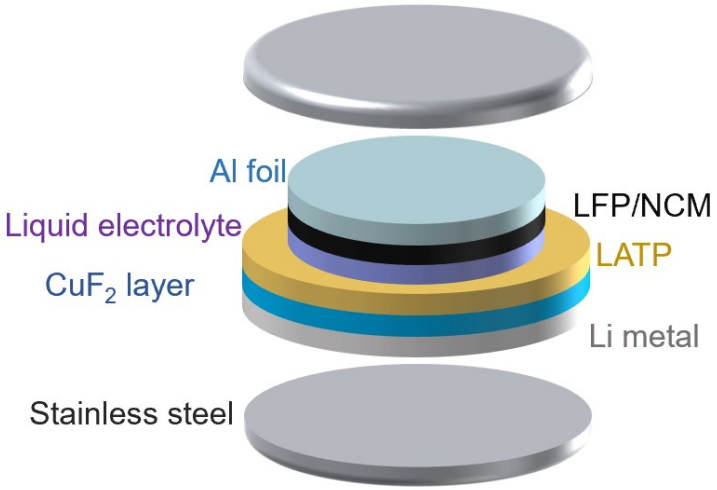

Figure S17. Full battery model.

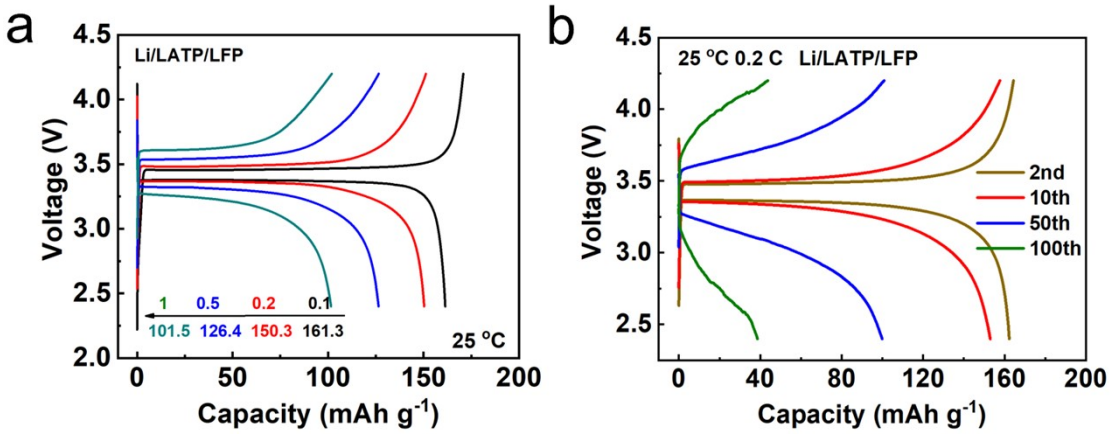

Figure S18. (a) Charge and discharge curves of Li/LATP/LFP full battery at different rates; (b) Charge and discharge curves of Li/LATP/LFP full battery at 0.2 C under different cycles.

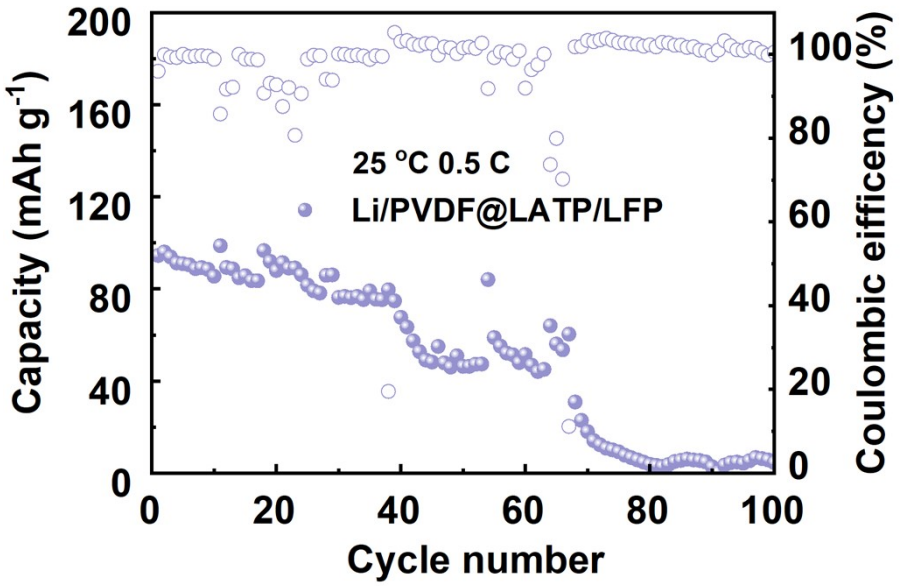

Figure S19. Cycling performance of the Li/PVDF@LATP/LFP full battery at 25 °C and 0.5 C.

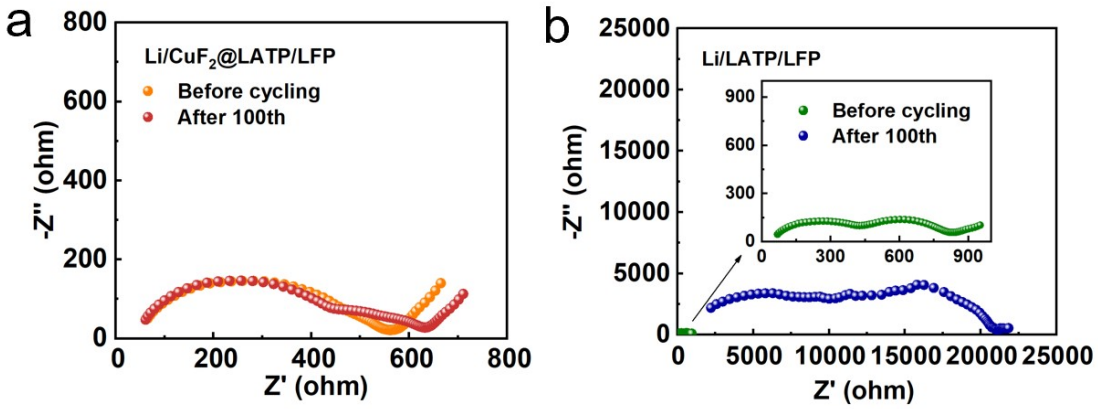

Figure S20. EIS curves of (a) Li/CuF_2@LATP/LFP and (b) Li/LATP/LFP full batteries before cycling and after 100 cycles at 0.2 C.

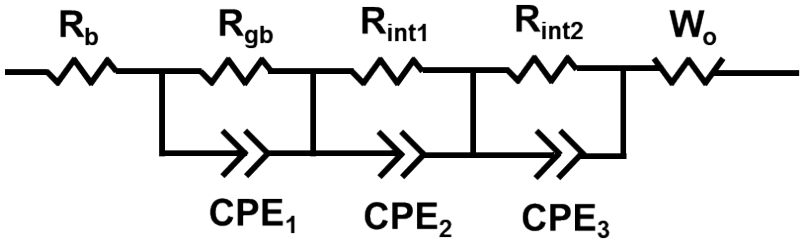

Figure S21. The equivalent circuit of full batteries.

The equivalent circuit of the full battery, where R_b represents the total resistance of the LATP, the intermediate layer, and the resistance of other components, including the electrode and the packaging material. R_{gb}, R_{int1}, R_{int2}, and W_o represent grain boundary resistance, interfacial resistance between positive electrode and electrolyte, interfacial resistance between negative electrode and electrolyte, and Warburg resistance, respectively.